Ultralight Wideband Open Boundary Quad-Ridged Antenna Manufactured Using 3D Printing Technology

Julien Haumant, Pierre Massaloux, Daouda Lamine Diedhiou, Alexandre Manchec, Rozenn Allanic, Cédric Quendo, Christian Person, Rose Marie Sauvage

Ultralight Wideband Open Boundary Quad-Ridged Antenna Manufactured Using 3D Printing Technology

J. Haumant[1,2], P. Massaloux [3], D. Diedhiou[1], A. Manchec[1], R. Allanic[2], C. Quendo[2], C. Person[4], R-M. Sauvage[5]
[1] Elliptika (GTID), 29200 Brest, France, Julien.haumant@elliptika.com
[2] Université de Bretagne Occidentale UMR6285, Lab-STICC, 29200 Brest, France
[3] CEA, CESTA, 33114 Le Barp, France
[4] IMT-Atlantique UMR6285, Lab-STICC, 29200 Brest, France
[5] DGA, 75000 Paris, France

***Abstract*—In this paper, authors propose to manufacture an ultra-wideband open boundary quad-ridged antenna using a 3D printing manufacturing method followed by a chemical metallization process. The lowest operating frequency has been decreased from 550 MHz to 300 MHz using dielectric slots. Furthermore, the structure of the antenna is optimized in term of weight and reached only 1100 g for an overall size of 442x442x442 mm^3. Finally, measurements show good performances over the frequency band from 300 MHz to 6 GHz.**

***Index Terms*— dielectric slots, lightweight, open boundary quad-ridged, ultrawideband antenna, 3D printing.**

I. INTRODUCTION

The huge expansion of wideband applications in military, wireless communication or biomedical domains, show that wideband antennas have become essential components in radiofrequency applications. Since the early of 1960's, the challenges associated to ultra-wideband antennas such as the radiation performances over the bandwidth, weight, compacity or cost have been widely studied [1]–[6]. Among all types of wideband antennas, the dual-ridged [1] and quad-ridged [2] antennas are commonly used and generally allow to achieve bandwidth up to 20:1.

The multiplication of wideband applications coupled with a need of higher performances seems to lead toward an increased complexity of RF structures. Consequently, new shapes of antennas are studied, conducting to longer development time, heavier devices, and thus higher cost.

This last decade, the emergence of plastic additive manufacturing techniques has carried out an important number of researches in radiofrequency devices: lens [7], waveguide slotted antenna [8], orthomode transducer [9] or front end device [10]. The wide accessibility of these rapid prototyping methods makes them an interesting alternative to conventional manufacturing techniques. Unlike conventional machining, 3D printing allows to manufacture extremely complex shapes with a minimum of constraints and development time.

The new degrees of freedom thus unlocked can be exploited to optimize the weight of structures without affecting radiofrequency performances as reported in [11] and [12]. In these articles, a waveguide and then a dual ridged horn antenna are completely perforated with electrically small holes which allowing to decrease drastically the global weight of the structure. Moreover, the usage of low volume density plastic materials in [12] minimizes the weight of radiofrequency devices.

In this paper, an open boundary quad-ridged antenna is first designed with conventional parameters. Then, dielectric slots are added on the flares and allow to increase the electrical length of the antenna, thus to decrease the lowest operating frequency. Finally, the shape of the antenna is optimized and perforated with electrically small holes to remove the maximum amount of material without affecting the mechanical integrity and the performances of the antenna.

II. ANTENNA CONCEPTION

A. Reference antenna

The reference antenna is designed according to conventional open boundary quad-ridged antennas which allow to achieve ultra-wideband performances from 550 MHz to 6 GHz. The exponential taper has proved its interests in wideband solutions for antennas [2], [13] and has been consequently chosen for the geometry of each flares. Regarding the considered manufacturing technique, the back cavity is circular which avoids any cantilevers surfaces as well as keeping the wideband matching of the antenna. The antenna is fed using two coaxial probes separated by a few millimeters to isolate the two orthogonal polarizations. The height, width and length of the body are equal to 442 mm. The design of the reference antenna and the feeding probes coaxial RG402 cables are shown in Fig. 1. The inner and the outer profiles of the ridges are terminated with a circularly shape. The profiles follow the values given in Tab. 1.

The antenna is simulated using the full-wave simulator HFSS™ and shows good matching results over the frequency band from 550 MHz to 6 GHz as presented in Fig. 2. However, the matching level under 700 MHz reaches -7 dB.

B. Bandwidth enhancement using dielectric slots

In this section, authors propose to increase the electrical length of the antenna by adding dielectric slots on each of flares.

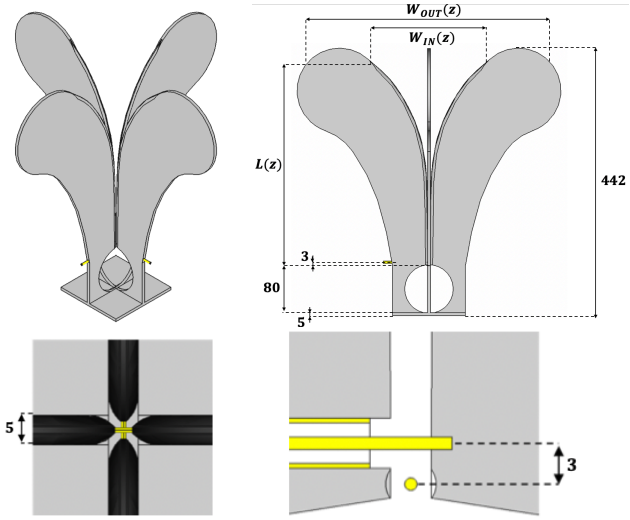

Fig. 1. Design and parameter given in mm of the reference antenna

TABLE 1. WIDTHS VALUES OF THE RIDGE ALONG THE ANTENNA

$L(z)$	$W_{IN}(z)$	$W_{OUT}(z)$
0	3	120
34	3	122
102	4.4	165
170	12	227
238	46	394
306	126.2	430
340	200	390

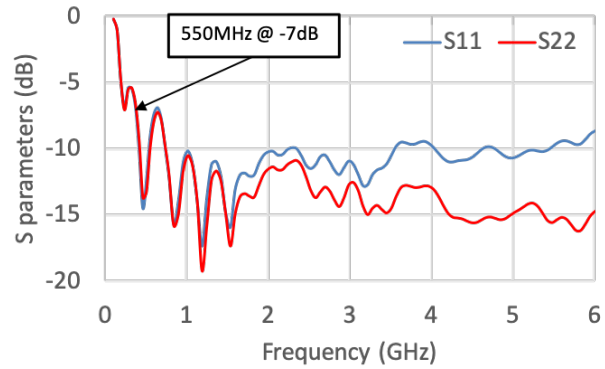

Fig. 2. Simulated scattering parameters of the reference antenna

This technique [13] applied on a planar Vivaldi antenna shows a reduction of the antenna size regarding to its lowest operating frequency. First, to keep mechanically strong structure and an easy printability, the slots height and width are respectively chosen to $H_{slot} = 10\ mm$ and $W_{slot} = 20\ mm$. The electrical properties of the dielectric material are fixed to $\varepsilon_r = 2.87$ and $\tan\delta = 0.027$ which correspond to the measured properties in S band (2.2 GHz – 3.3 GHz) of the used resin.

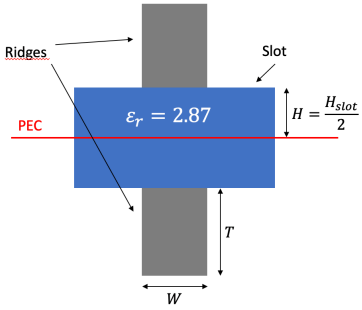

Fig. 3. Model of the microstrip line approach for the determination of the effective permittivity

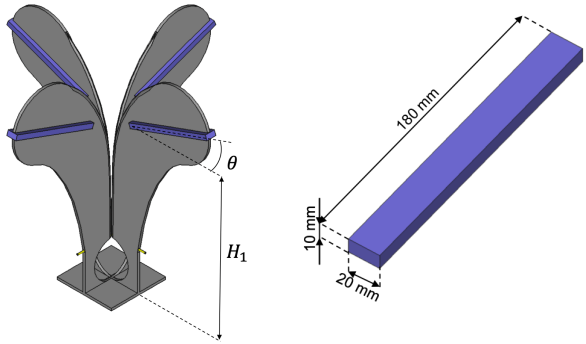

Fig. 4. Design and parameters of the antenna with the dielectric slots

The slots will resonate at the frequency where their lengths are equal to a quarter of the guided wavelength. Since the local structure is in a mixed medium, the challenge is to determine the effective permittivity seen by the wave inside the slots in order to calculate its length. As an approach to get an initial value for the electromagnetic optimization, the problem is solved as a microstrip transmission line as shown in Fig. 3. The slots inserted inside the two ridges can be seen as a substrate where two opposed and thick microstrip lines are separated by a perfect electrical conductor (PEC). The effective permittivity can be calculated using the transmission line impedance tool *LineCalc (ADS)*. The thickness of the line is restricted to 4.99 mm due to the model limitation ($T < W = 5\ mm$) but it should be sufficient to get an approximate value of the effective permittivity. The effective permittivity calculated on *LineCalc* ($\varepsilon_r = 2.87\ ; H = 5mm\ ; W = 5\ mm\ ; T = 4.99\ mm$) is equal to $\varepsilon_{reff} = 2.01$ and leads to the following slots length l_{slot}:

$$l_{slot} = \frac{c}{4f\sqrt{\varepsilon_{reff}}} = 176\ mm$$

Where c, the speed of light in vacuum and f the desired resonant frequency (300 MHz).

The length of the slots after optimization are changed to 180 mm which gives better results. The slots have been placed at $H1 = 322\ mm$ height from the bottom of the antenna and tilted by $\theta = 20\ degrees$ (They cannot be place horizontally due to insufficient space). The design of the antenna with the slots is shown in Fig. 4.

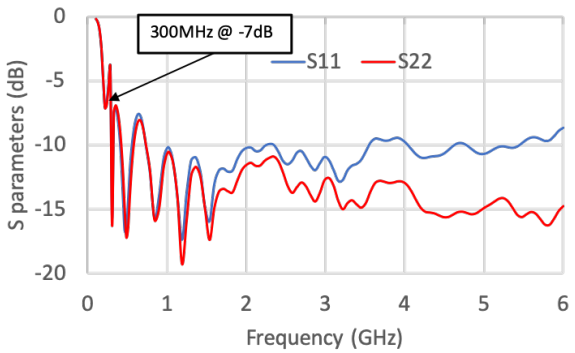

Fig. 5. Simulated scattering parameters of the antenna with the dielectric slots

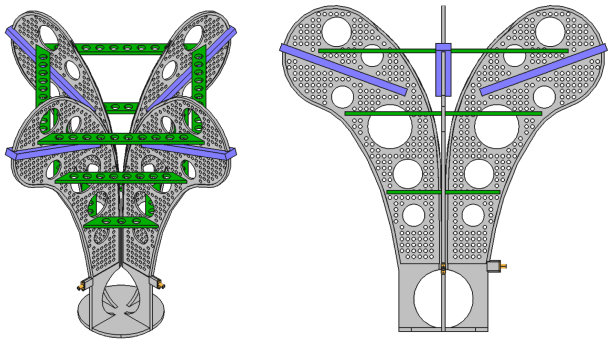

Fig. 6. Design of the final body of the antenna with all perforations

The simulated scattering parameters response is shown in Fig. 5. The results show that dielectric slots have induced a new resonance and allow the antenna to operate from 300 MHz.

C. *Weight optimisation and mechanical considerations*

The low volume density of most plastic materials is commonly used to decrease the global weight of a structure. As an example, the resin used to print the structure is around 1.1 g/cm^3 against 2.7 g/cm^3 for aluminum. Most of all, the flexibility of 3D printing allows to modify the structure easily in order to remove a huge amount of materials without disrupting antenna performances and maintaining a strong mechanical structure.

The weight of the proposed antenna is drastically decreased by perforating the structure with multiple holes of different sizes. The small holes are designed to have a neglectable impact at the shortest wavelength at 6 GHz. The diameter of these holes is equal to 5 mm which correspond to 0.1 λ at 6 GHz. Then bigger holes (30 mm to 60 mm of diameter) are added in order to remove a higher volume of material. They are placed in the center of each ridge where the current density is lower than on their sides. In this way, it should have lower impact on the response. The volume of material for the final antenna shown in Fig. 6 is around 430 cm^3 against 895 cm^3 for the reference antenna.

The simulated realized gain as a function of the frequency is presented in Fig. 7 for the antenna without holes, the antenna with the small holes, and the antenna with the small and big holes. The small holes reduce the realized gain at high frequencies above 5.5 GHz and the big ones above 1 GHz

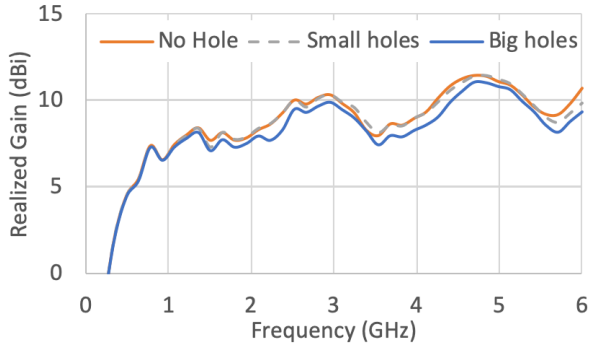

Fig. 7. Simulated realized gain of the final antenna

(a) (b)

Fig. 8. Photographs of (a) the printed antenna; (b) one of the printed dielectric slot

where it is slightly lower in the privilege radiation direction. The final realized gain varies from 1.5 dBi at 300 MHz to a maximum of 11 dBi.

The low mechanical properties of the plastic, compared to aluminum ones, can cause deformations at different steps of the manufacturing process due to the large dimensions of the antenna. Thus, several non-metallized structures are added as shown in green color in Fig. 6 and allow to keep the flares at a good distance from each other. These non-metallized structures are placed in order to limit the radiation perturbations and have not shown any noticeable impact on the scattering parameters response.

III. Manufacturing Details

The antenna is manufactured in one piece using an SLA printer. The electrical properties of the resin are unknown, nevertheless, this resin has been used for purely mechanical purposes by being fully metallized.

The slots are also manufactured with an SLA printer, therefore, the complex permittivity of the resin has been measured in S-band (2.2 GHz – 3.3 GHz) with a transmission line waveguide method and is equal to $\varepsilon_r = 2.87$ and $\tan\delta = 0.027$. The printed antenna and slots are shown in Fig. 8.

The antenna is then metallized using the conventional chemical deposition reported in [14] on a slotted coaxial line: (i) surface roughness enhancement by dry sandblasting, (ii) palladium catalysis, (iii) 3 µm chemical copper deposition, (iv) 10 µm electrolytic copper deposition and (v) 10 µm

(a) (b)

Fig. 9. Photographs of the (a) printed antenna after the metallization process; (b) mechanical structures to rectify the deformations

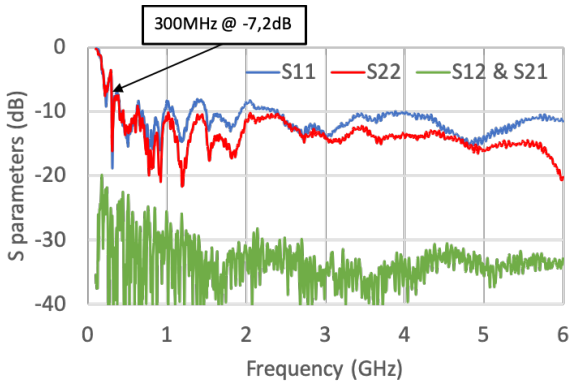

Fig. 10. Measured scattering parameters of the manufactured antenna

electrolytic tin deposition. The significant thickness of the tin deposition is not mandatory, especially because the conductivity of tin is lower than the copper one. However, the large scale of the antenna makes an inhomogeneous thickness of deposition. The time in the electrolytic bath are thus increased and ensure a minimal thickness of tin on all surfaces. The selective metallization is done using pieces of tape. The final body is shown in Fig. 9 (a).

However, due to the temperature of the metallization bathes ($\approx 40\,°C - 50\,°C$), the flares of the antenna undergo deformations, especially on the slots and the base of the antenna where the feeders are placed. In order to rectify the structure, several non-metallized small pieces are added as shown in Fig. 9 (b).

The final body measured weight comprising all slots and mechanical parts is equal to 1100 g which is light compared to the size of the antenna.

IV. Measurements

The scattering parameters of the manufactured antenna are shown in Fig. 10. The two polarizations are matched under -10 dB on the most part of the frequency band, however, few peaks reached -7 dB in the lowest frequencies' region. The coupling between the two polarizations varies from -24 dB to -40 dB over whole the bandwidth.

V. Conclusion

An ultra-wideband quad-ridged antenna in the frequency band from 300 MHz to 6 GHz is manufactured using a stereolithography printing method followed by a selective metallization process. Four 3D printing dielectric slots have been added and allow to reduce the size of the antenna compared to its lowest operating frequency. The final body' volume is 442x442x442 mm^3 and the optimization of the structure maintains the weight lower than 1100 g. Finally, measurements are in good agreement with the simulations and present a global matching level lower than -10 dB with some regions at -7 dB at the lowest frequencies.

References

[1] R. Chatterjee et J. Y. Siddiqui, « Compact design of an UWB dual ridged horn antenna », in *2013 IEEE Applied Electromagnetics Conference (AEMC)*, déc. 2013, p. 1-2, doi: 10.1109/AEMC.2013.7045119.

[2] Z. Wenliang, Q. Jinghui, et S. Xianqing, « Quad-ridge dual polarized horn antenna design and optimization », in *Proceedings of 2014 3rd Asia-Pacific Conference on Antennas and Propagation*, juill. 2014, p. 643-646, doi: 10.1109/APCAP.2014.6992577.

[3] H. Ravichandran, J. V.M., et S. N. Rao, « A Dielectric Filled Dual Ridged Horn Antenna(DFDRHA) for Ultra-Wideband Applications », in *2019 3rd International conference on Electronics, Communication and Aerospace Technology (ICECA)*, juin 2019, p. 1076-1080, doi: 10.1109/ICECA.2019.8822201.

[4] V. Rodriguez, « Open boundary quadridge horn antenna for the 80 MHz to 1 GHz range: A dual polarized solution for testing antennas in the VHF and UHF ranges », in *Proceedings of the Fourth European Conference on Antennas and Propagation*, avr. 2010, p. 1-4.

[5] G. Cortes-Medellin, « Controlling the gain of wide band open quad ridge antennas », in *12th European Conference on Antennas and Propagation (EuCAP 2018)*, avr. 2018, p. 1-3, doi: 10.1049/cp.2018.1229.

[6] L. Chang, L.-L. Chen, J.-Q. Zhang, et D. Li, « A 1.95-19.35 GHz Quad-Ridge Horn Antenna with Stable Unidirectional Radiation Patterns », in *2018 12th International Symposium on Antennas, Propagation and EM Theory (ISAPE)*, déc. 2018, p. 1-3, doi: 10.1109/ISAPE.2018.8634279.

[7] B. Zhang *et al.*, « A K-Band 3-D Printed Focal-Shifted Two-Dimensional Beam-Scanning Lens Antenna With Nonuniform Feed », *IEEE Antennas Wirel. Propag. Lett.*, vol. 18, nº 12, p. 2721-2725, déc. 2019, doi: 10.1109/LAWP.2019.2950264.

[8] K. Zhao, G. Senger, et N. Ghalichechian, « 3D-Printed Frequency Scanning Slotted Waveguide Array with Wide Band Power Divider », in *2019 United States National Committee of URSI National Radio Science Meeting (USNC-URSI NRSM)*, janv. 2019, p. 1-2, doi: 10.23919/USNC-URSI-NRSM.2019.8712999.

[9] M. García-Vigueras *et al.*, « Mm-wave antennas and components: Profiting from 3D-printing », in *2017 International Conference on Electromagnetics in Advanced Applications (ICEAA)*, sept. 2017, p. 1016-1020, doi: 10.1109/ICEAA.2017.8065432.

[10] F. L. Borgne, G. Cochet, J. Haumant, D. Diedhiou, K. Donnart, et A. Manchec, « An Integrated Monobloc 3D Printed Front-end in Ku-band », in *2019 49th European Microwave Conference (EuMC)*, oct. 2019, p. 786-789, doi: 10.23919/EuMC.2019.8910891.

[11] G.-L. Huang, S.-G. Zhou, C.-Y.-D. Sim, T.-H. Chio, et T. Yuan, « Lightweight Perforated Waveguide Structure Realized by 3-D Printing for RF Applications », *IEEE Trans. Antennas Propag.*, vol. 65, nº 8, p. 3897-3904, août 2017, doi: 10.1109/TAP.2017.2715360.

[12] J. Haumant, et al., « Ultralight Wide-band Double Ridged Horn Antenna Using AdditiveTechnologies », *Microwave Technology and Techniques Workshop (MTT'19)*, Noordwijk, Nehterlands, 2019.

[13] M. Y. Perdana, T. Hariyadi, et Y. Wahyu, « Design of Vivaldi Microstrip Antenna for Ultra-Wideband Radar Applications », *IOP Conf. Ser. Mater. Sci. Eng.*, vol. 180, p. 012058, mars 2017, doi: 10.1088/1757-899X/180/1/012058.

[14] J. Haumant *et al.*, « Ultra Wideband Transition From Coaxial Line to Two Parallel Lines Manufactured Using Additive Manufacturing Technology », in *2019 IEEE MTT-S International Microwave Symposium (IMS)*, juin 2019, p. 1217-1220, doi: 10.1109/MWSYM.2019.8701001.